Overview of Crack Visualization Process

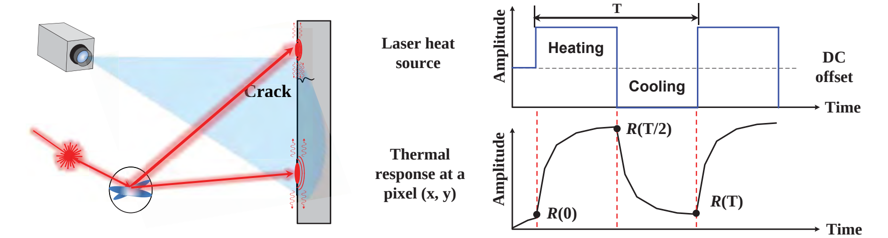

Lock-in amplitude image

$A(t) = \sqrt{[\{R(0) - R(T/2)\}^2 + \{R(T/2) - R(T)\}^2]}$

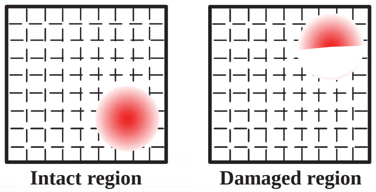

Crack visualization based on Holder exponent & Extreme value analysis

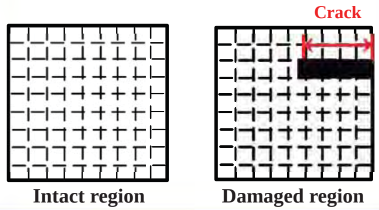

Experimental Setup for Laser Lock-in Thermography

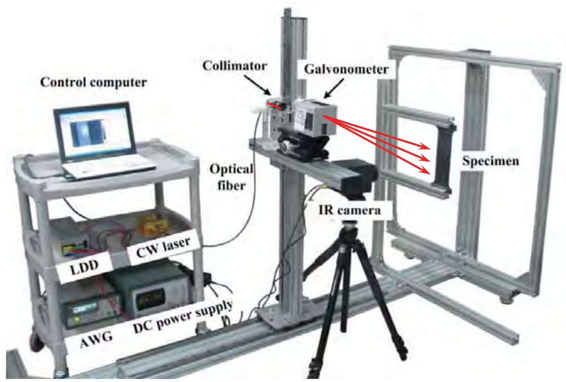

CW Laser
- **Wavelength**: 808 nm
- **Waveform**: Square signal
- **Frequency**: 100 mHz
- **Power**: 3.8 W
- **Beam diameter**: 15 mm

IR Camera
- **Spatial resolution**: 640 x 480 pixels
- **Sampling frequency** : 50 Hz
- **Temperature resolution**: 0.03 K
- **Wavelength**: 7.5 to 14 μm

Galvanomirror
- **Rotating speed**: 5730 °/s
- **Maximum Scanning angle**: ±21.8 °
- **Angular resolution**: 6.6 x 10^{-4}

Crack Localization and Quantification using Laser Lock-in Thermography

Laser point scanning scheme for fatigue crack evaluation

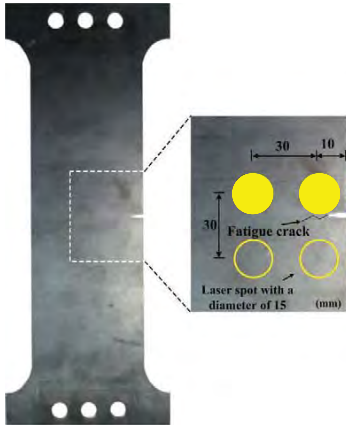

Crack Length Estimation

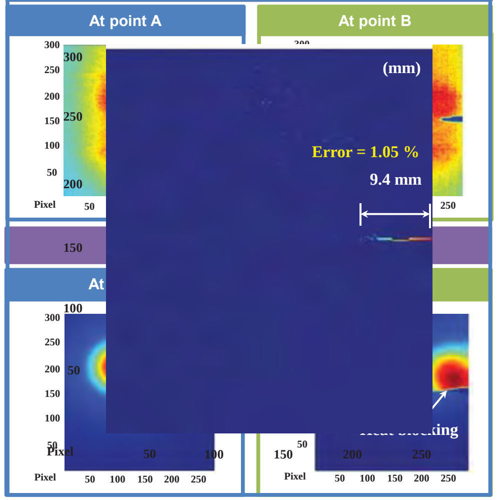

* Y.K. An, J.M. Kim, H. Sohn, *NDT & E International*, accepted, 2014

Fatigue Crack Detection in a Welded Joint

Laser point scanning scheme for crack evaluation in welded joint

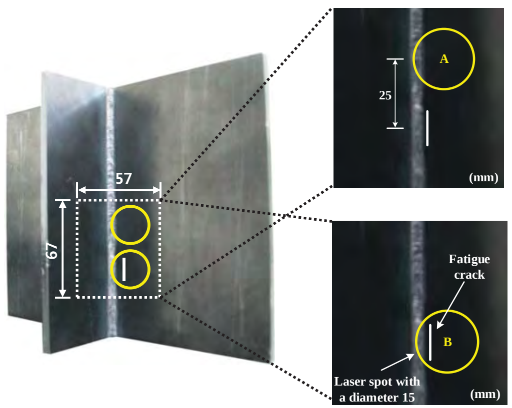

Holder exponent image

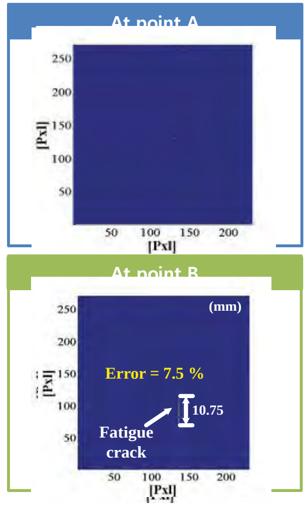

* Y.K. An, J.M. Kim, H. Sohn, *NDT & E International*, accepted, 2014

Online Inspection of Semiconductor Die Chip using Laser Lock-in Thermography (Sponsored by Samsung Electronics)

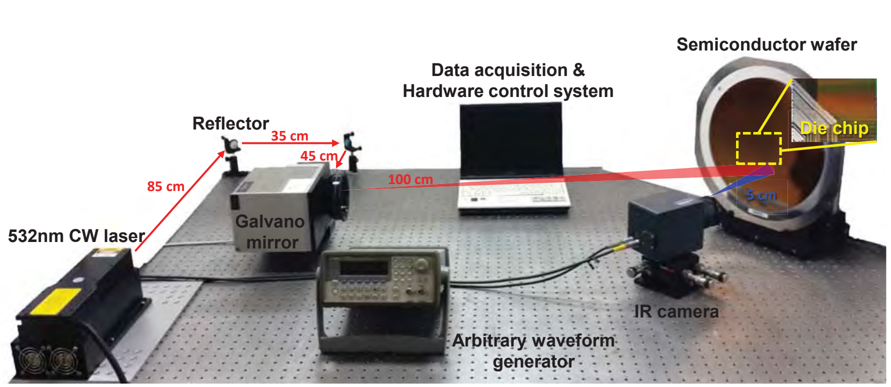

CW Laser	IR Camera	Galvanomirror
Wavelength: 532 nm	**Temperature resolution**: 0.03 K	**Rotating speed**: 5730 °/s
Beam diameter: 4 mm	**Wavelength**: 7.5 to 14 μm	**Angular resolution**: 6.6 x 10^{-4}

* Y.K. An, J.M. Kim, H. Sohn, *Proc. SPIE 8692, Sensors and Smart Structures Technologies for Civil, Mechanical, and Aerospace Systems*, 2013

Manufacturing Process of Semiconductor Die Chips

Front

Back lap
- Grind wafer until a tens of μm thickness
- Cover Lamination tape

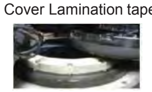

Wafer saw
- Cut the wafer into an individual chip

Die attach & Cure
- Attach individual chip on a substrate by using adhesives
- Curing step
  :one hour in 175℃
  :or two separated steps in 125 ℃ ~ 175 ℃

Wire bonding
- Connect the chip and lead frame with gold wire

Die chip cracks are often produced during wafer back-grinding process

Back-grinding is a semiconductor device fabrication step during which wafer thickness is reduced to allow for stacking and high density packaging of integrated circuits using a rotational grinder.

- Curing step
  : 1 hr ~ 5 hr in 175 ℃
- : different set-up temperatures at different sections (190 ℃~280 ℃)

Test

TDBI (Test During Burn-In) test
- Separate defective products
- Maximum temperature: 125 ℃

Tests for electric features and functionality
- Temperature range: -5 ℃ ~ 90 ℃

Semiconductor Chip Crack Visualization using Line Source Laser Beam

- **Damaged chip sample I (crack width: 20~30 μm)**

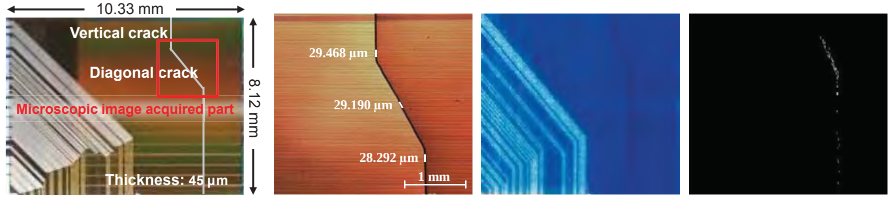

Test sample (Chip type 1) | Microscopic image | Raw image | Final image

- **Damaged chip sample II (crack width: 30~40 nm)**

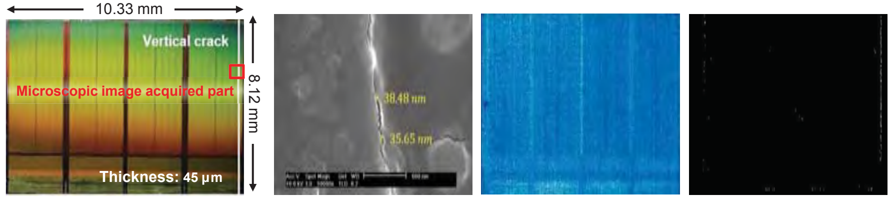

Test sample (Chip type 2) | SEM image | Raw image | Final image

Semiconductor Chip Crack Visualization using Simultaneous Multipoint Excitations

- **Damaged chip sample III (vertical crack)**

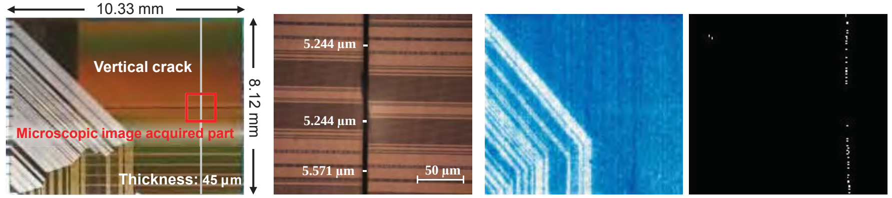

Test sample (Chip type 1) | Microscopic image | Raw image | Final image

- **Damaged chip sample IV (horizontal crack)**

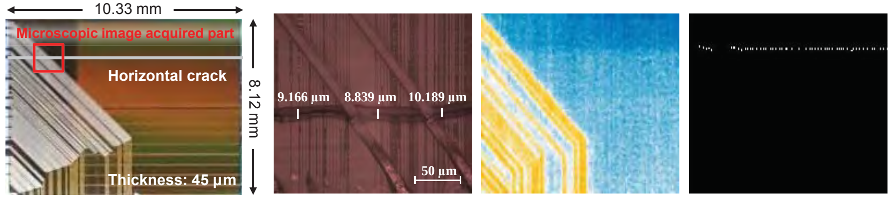

Test sample (Chip type 2) | Microscopic image | Raw image | Final image

Presentation Outline

1. **Noncontact Laser Ultrasonics**
   - Notch detection for metallic structures
   - Delamination detection for composite & wind turbine structures
   - Fiber guided laser ultrasonic system for nuclear power plant monitoring
2. **Contact/Noncontact Nonlinear Ultrasonic Wave Modulation**
   - PZT based crack detection for an aircraft fitting lug
   - ACT based crack detection for a rotating shaft
   - Laser based nonlinear ultrasonics wave modulation
3. **Laser Lock-in Thermography**
   - Surface crack detection for high-speed train bogies
   - Micro crack detection for semiconductor chips
4. **LiDAR/LADAR**
   - Noncontact dynamic displacement estimation
   - Dimension estimation for precast concrete slabs
   - Surface defect detection for concrete panels
5. **Laser based Power/Data Transmission**

Working Principle of LiDAR/LADAR

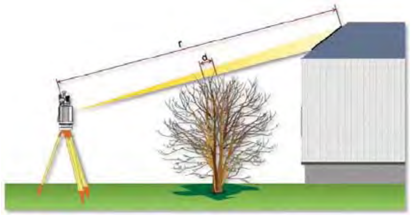

Figure from Riegl Inc.

Time of Flight Type

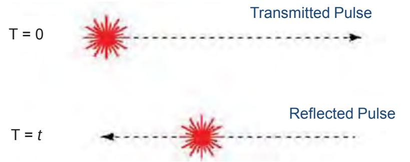

- Built-in clock directly measures travel time laser pulses and convert it to distance.
- 1 mm of accuracy and 3 mm of precision
- Long measurement distance (~ 3 km)

Phase Shift Type

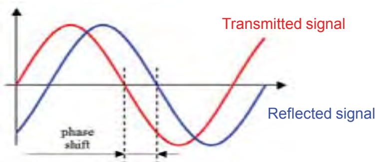

- Incident continuous sinusoidal laser beam and reflected beam are compared for phase shift
- 0.3 mm of accuracy and 2 mm of precision
- Short measurement distance (~120 m)

➡ Limited displacement accuracy of 0.3 mm to 1 mm and low sampling rate of less than 10 Hz

Dynamic Displacement Estimation using LDV/LiDAR
(Sponsored by Korea Ministry of Land, Infrastructure & Transport)

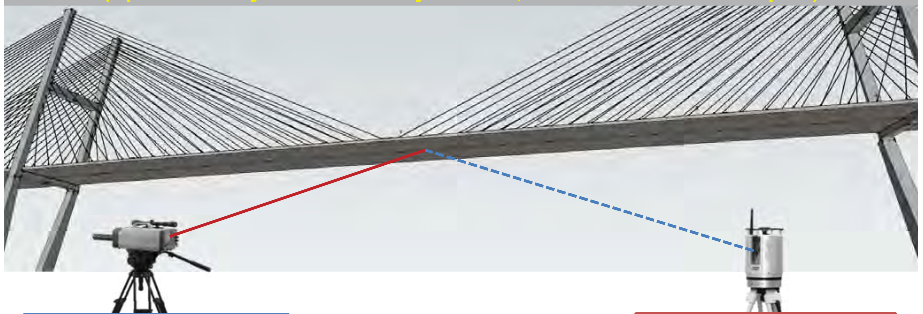

Velocity measurement by LDV

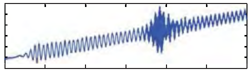

- High frequency (up to 4 MHz)
- High accuracy (< 0.1 μm/s)
- Measures velocity (integration needed and error accumulation unavoidable)

Dynamic displacement estimation using two-stage Kalman filter

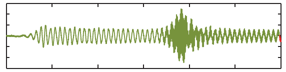

- High frequency (< 4 MHz)
- High accuracy (< 50 μm)
- No integration error

Displacement measurement by LIDAR

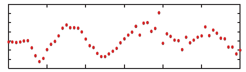

- Low frequency (< 120 Hz)
- Low accuracy (< 3 mm)
- Directly measures displacement (no integration error)

* J. Kim, K.Y. Kim, H. Sohn, *Mechanical Systems and Signal Processing*, Vol. 42, PP. 194-205, 2014

Dynamic Loading Test for Bridge Rating (In collaboration with Prof. H.K Kim at SNU, N.S. Kim at Pusan Univ., J.H. Kim at Dankook Univ.)

Yeondae Br. Jungbu Expressway, South Korea

- Experimental test bridge built on Jungbu Inland Expressway, Korea, 2002
- Steel box girder bridge
- Total length 180m (45m@4 spans)
- Total 12 loading cases with different truck speeds (10, 60, 100 km/h)

LVDT (Linear Variable Differential Transformer)

- Used as reference
- Fixed on complex support
- Sampling rate – 100Hz

LDV and LiDAR

LDV (velocity measurement, 1280Hz sampling rate)

LiDAR (displacement measurement, 120Hz sampling rate)

Test Results for Dynamic Displacement Estimation

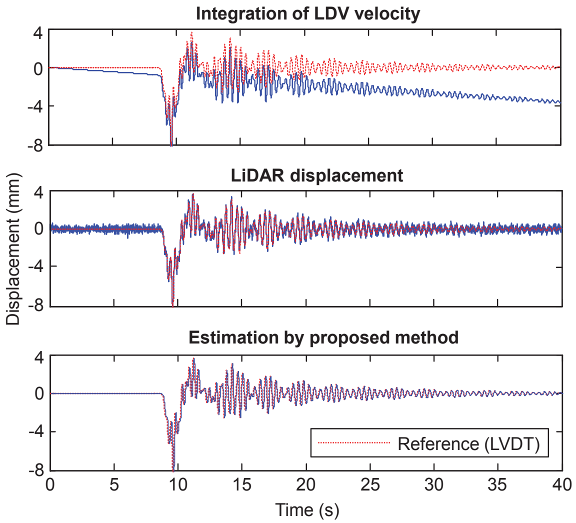

Loading cases #	RMS error (mm)
1	0.0319
2	0.0403
3	0.0385
4	0.0494
5	0.0334
6	0.0343
7	0.0563
8	0.0546
9	0.0544
10	0.0647
11	0.0550
12	0.0464
Average	0.0466

Dimension Estimation for Precast Concrete Slabs using LiDAR
(Sponsored by Korea Ministry of Land, Infrastructure & Transport)

LiDAR based Precast Concrete Slab Inspection


Modularized Precast Components

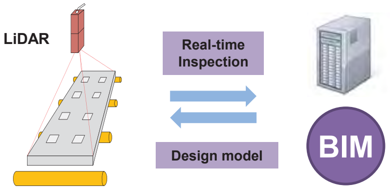

System Overview

(1) Dimensional Estimation

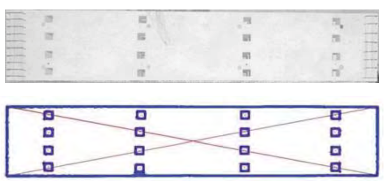

(2) Flatness Estimation

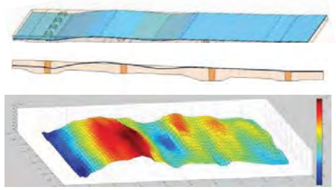

In-Situ Inspection of Real Precast Concrete Slabs


Experiment setting in construction area


3D Scanner setting

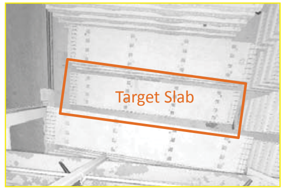

Top scanning view

Dimension Inspection Results

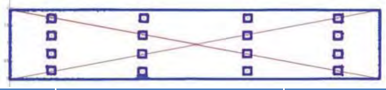

Angular Resolution	Dimension Error(mm)				Position Error(mm)	
	Length (Slab)	Width (Slab)	Length (SP)	Width (SP)	Length (SP)	Width (SP)
0.072	2.3	25.6	4.1	16.0	3.8	19.4
0.036	2.7	7.3	6.2	9.0	5.7	9.6
0.018	1.0	4.7	6.6	5.8	5.3	7.6

Flatness Inspection Results

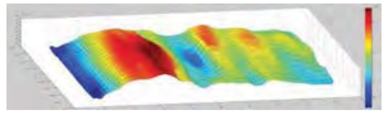

Discrepancy (mm)			Area Percentage	
max	min	average (abs value)	discrepancy >5 mm	discrepancy <-5 mm
9.4	-8.0	2.0	4.1%	4.1%

* M.K. Kim, H. Sohn, and C.C. Chang, *Proceedings of Computing in Civil Engineering*, PP. 621-628, 2013

Surface Defect Characterization for Concrete Panels

Test Setup

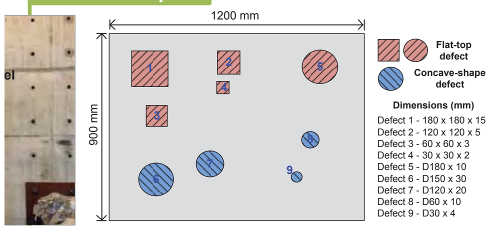

Panel Specification

Test Setting

Test Results

Defect Visualization

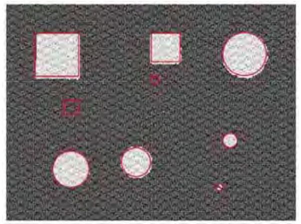
Defect Classification

Presentation Outline

1. **Futuristic View of Infrastructure Monitoring**
2. **Noncontact Laser Ultrasonics**
   - Notch detection for metallic structures
   - Delamination detection for composite & wind turbine structures
   - Fiber guided laser ultrasonic system for nuclear power plant monitoring
3. **Contact/Noncontact Nonlinear Ultrasonic Wave Modulation**
   - PZT based crack detection for an aircraft fitting lug
   - ACT based crack detection for a rotating shaft
   - Laser based nonlinear ultrasonics wave modulation
4. **Laser Lock-in Thermography**
   - Surface crack detection for high-speed train bogies
   - Micro crack detection for semiconductor chips
5. **LiDAR/LADAR**
   - Noncontact dynamic displacement estimation
   - Dimension estimation for precast concrete slabs
   - Surface defect detection for concrete panels
6. **Laser based Power/Data Transmission**

Wireless Power and Data Transmission for Guided Wave Generation and Sensing

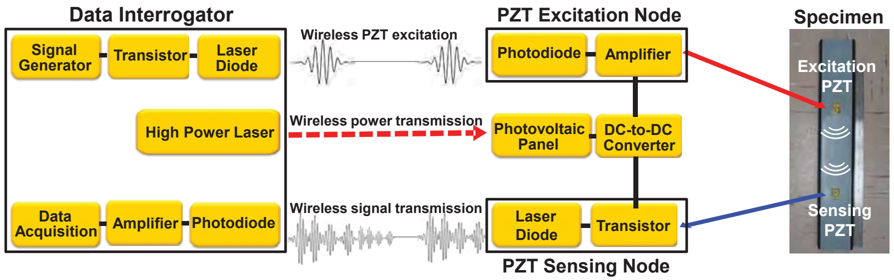

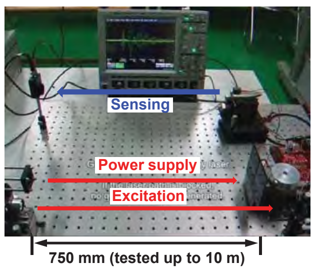

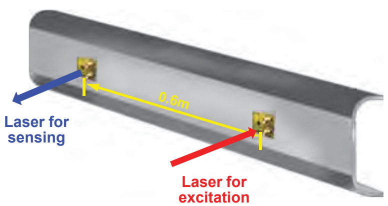

* H.J. Park, H. Sohn, C.B.Yun, et al., *Smart Materials and Structures*, Vol. 21, 035029(10pp), 2012

Wireless Power and Data Transmission for Remote E/M Impedance Measurement

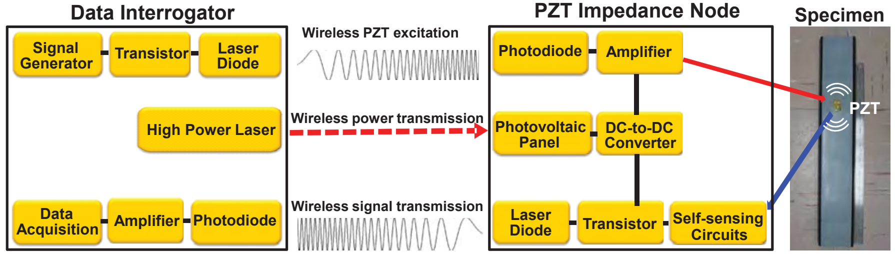

PZT Impedance Node

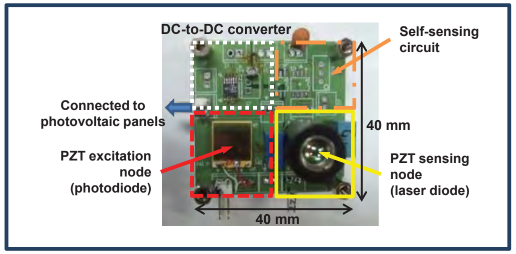

* H.J. Park, H. Sohn, C.B. Yun, et al., *Smart Materials and Structures*, Vol. 21, 035029, 2012

Conclusions

- **Noncontact laser sensing techniques will have its own fair share in future SHM and NDT applications mainly due to the following advantages**
  - **Achievement of high spatial resolution**
  - **Rapid deployment without or few sensor placements**
  - **Time and cost reduction in sensor installation, cabling and maintenance**
  - **Improved the overall system (target structure + sensors) reliability**
  - **Application to moving targets and under harsh environments**
- **However, there are still many technical hurdles that need to be overcome before these techniques can be transitioned to commercialization.**
  - **Eye safety issue**
  - **Alignment and control of laser beam**
  - **Often special surface treatment is necessary for LDV**
  - **Limited applicability to structures with complex geometries**

Acknowledgements (Collaborators)

- C.B. Yun, H. Myung, H.J. Jung , J.W. Hong at KAIST
- H.K Kim at Seoul National University
- N.S. Kim at Pusan University
- J.H. Kim at DanKook University
- H.W. Park at Dong-A University
- K.H. Park at EM4SYS and GIST
- M. Derriso, Kevin Brown at US Air Force Research Laboratory
- M.P. Desimio, S.E. Olson at UDRL
- E. Swenson at US Air Force Institute of Technology
- T. Kundu at University of Arizona
- J.P. Lynch at University of Michigan
- W. Wang at Northeastern University
- C.C. Chang and J. Chen at Hong Kong University of Science and Technology
- Z. Su at Hong Kong Polytechnic University
- P. Masson at Université de Sherbrooke
- W. Ostachowicz at Institute of Fluid Flow Machinery, Polish Academy of Sciences

Acknowledgements (Funding Agencies)

- Mid-career Researcher Program at the National Research Foundation of Korea (NRF) funded by the Ministry of Education, Science and Technology
- A grant from EEWS Research Project of the office of KAIST EEWS Initiative
- Korea Institute of Energy Technology Evaluation and Planning
- Korea Ministry of Knowledge Economy
- Asian Office of Aerospace Research and Development (AOARD)
- Ministry of Land, Infrastructure and Transport of Korean government
- Air Force Research Laboratory, USA
- Samsung Electronics, Korea
- Hyundai/KIA Motors, Korea